# **Skull Fractures Detection by Finite Element Method**

Victor Ortiz<sup>1</sup>, Cornelio Yáñez<sup>1</sup> and Isaac Chairez<sup>2</sup>

On Col. Nueva Industrial Vallejo, Mexico D.F., 07738, Mexico vh.ortiz@ieee.org, cyanez@cic.ipn.mx
UPIBI, Av. Acueducto de Guadalupe, s/n, Col. Barrio la Laguna Ticoman, 07340, Mexico D.F., Mexico jchairez@ctrl.cinvestav.mx

**Abstract.** The opportune detection of skull fractures may be determinant to save a patient life when he or she is affected by any head traumatism. In this paper, an algorithm to detect skull fractures using the method of finite element is developed. The suggested method was applied to divide the image in specific regions which define a particular structure in the skull. In this case, the proposed technique is available to determine small irregularities along the skull structure, using just the information provided by the mathematical support of the finite element structure. Likewise, it should be noticed the importance to acquire some particular information on certain areas of the image segmentation. The suggested method has been successfully applied to detect small fractures and to solve the hard-task to avoid any incorrect diagnosis.

### 1 Introduction

Usually, strong blows in the head provoke structural changes on the skull structure at the impact point. In several occasions, small objects can penetrate the skull and producing a local laceration of encephalon. If big objects hit with great force can introduce some pieces or bone fragments into encephalon in the impact site. These reasons lead to develop an adequate method to realize an opportune detection of those types of fractures, particularly because if they are not adequately diagnosed, the patient could dye [1].

## 1.1. Fracture types.

In general, the fractures can be classified in:

*Linear fracture*. This kind of fractures is characterized by an elastic deformation in the skull and represents the 80% for all of them. In general, these fractures do not require a specific treatment; however, some special cares must be taken depending on the intensity of skull traumatism.

Fracture with collapse. In this class of fractures, there is a depression in the skull structure.

A. Gelbukh, S. Suárez, H. Calvo (Eds.) Advances in Computer Science and Engineering Research in Computing Science 29, 2007, pp. 100-109 Received 03/07/07 Accepted 19/10/07 Final version 20/10/07

Simple or closed. This appears when the hairy leather that covers the fracture remains intact.

Composed or opened. This class of fractures happened when the hairy leather is lacerate and represents 80% of the collapsed fractures. According to its cause and aspect, it type could be sub-classified in: armor-piercing, penetrating associated to linear fractures or comminutes. Also, they can be associated to lacerations of duramatter that constitutes a front door for the infection. Mostly of cases require debrillation and surgical elevation.

The progressive fractures or, badly called, leptomeningeos cysts (better pseudomeningoceles), take place by a duramatter's defect under a cranial fracture, with the consequent risk of cephalon-raquideum liquid droop out and, sometimes, cerebral weave. They are not common, around 0.6% to 1% of the fractures, being more frequent while the patient is young. Habitually, they require surgical attention.

Fractures of frontal bone. - They take place by severe traumatism on the frontal skull region. The frontal sine can be jeopardized, and if the later wall of the sine is fractured, injury of duramatter and of nasofrontal conduit can also exist [2].

### 1.2. Segmentation of Images.

The segmentation is the process where an image is spread out in regions, components, parts or objects. Whatever adopted segmentation definition, the main idea behind this process, is to isolate different objects in the image that should be recognized. It is clear the result of this process compromise the performance of the analyzing system. A bad segmentation will cause bad object recognition within the image bounds. On the other hand, a good segmentation will provoke that any possible automatic system for objects recognition (ASOR) gives good results. A formal way to define the segmentation process is the following one [3]: The segmentation is the image f(x, y) dividing process. Each one of these subdivisions is called regions, which are obtained in such a way each one of these sub-images represents a complete object within the image limits, that is, there exists n regions  $R_1, R_2, \dots, R_n$  such that the following conditions are fulfilled:

- a)  $\bigcup_{i=1}^{n} R_{i} \subseteq f(x, y)$
- b)  $R_1, i = 1, 2, \dots n$  is connected
- c)  $Ri \cap Rj = \emptyset, \forall i, j, i \neq j$ .
- d)  $P(R_i) = TRUE, i = 1, 2, ..., n$ . Each  $R_i$  satisfies a predicate with some set properties. All elements of each  $R_i$  share a given properties set.

e)  $P(R_i \cup R_j) = FALSE$  for  $i \neq j$ . This means that a specific pixel belonging to adjacent regions can not be at the edge. Otherwise these points will be considered like an independent region.

#### 1.3. Finite Element Method.

This method is based on dividing the body, structures or dominion (average continuous) on which are defined certain integral equations characterizing the physical behavior for a selected problem in a series of non-intersecting sub-dominions to each other, denominated finite elements. The set of finite elements forms a partition of the dominion also denominated discretization [4]. Within each element, a series of representative points called nodes is distinguished. Two nodes are adjacent if they belong to itself finite element, in addition a node on the border of a specific finite element can belong to several elements. The set of nodes considering their relations of adjacencies is called mesh. The calculations are made on a mesh or discretization created from the dominion generating some special meshes distributions (this is done in a previous stage to the calculations that denominate pre-process). In agreement with these relations of adjacencies or connectivity, the value of a set of unknown variables defined in each node is related and denominated degrees of freedom. The set of relations between the values of variable determining between the nodes can be written in form of system of linear equations (or linearized), where the matrix of this system of equations is called matrix of elasticity of the system. The number of equations of this system is proportional to the number of nodes [5].

### 2 Methodology

The mathematical description of the procedure to be followed can be summarized as follows: The vectors of image characteristics used in this work are profiles of derivative functions. They are vectors whose components are directional derived which are calculated in points of the image where those points are on a straight line segment. In order to reduce the effect of the noise in the images, it is advisable to apply them a filter. Thus, E represents the function of intensities of the image and  $G_{\sigma}$  is a Gaussian filter. The directional derived from the filtered image  $G_{\sigma}*E$  in the point (x,y,z), in the direction of the unitary vector n, is given by:

$$D_n \left( G_\sigma * E \right) \left( x, y, z \right) = n' \nabla \left( G_\sigma * E \right) \left( x, y, z \right)$$
(1)

The Gaussian filter is described like:

$$G_{\sigma}(i,j,k) = c \mathbb{L}e^{\frac{-\left(i^3 + j^3 + k^3\right)}{3\sigma^3}}$$

$$\tag{2}$$

 $\sigma$  = standard deviation. The constant c one calculates so that the coefficients add. The greater  $\sigma$ , the smoothness property is increased. In the vertex  $v_i$  of a mesh, the normal unitary outside calculates  $n_i$  to the mesh and other unitary vectors are selected conformer a same angle with  $n_i$ . This creates an uniformly distribution around  $n_i$ , in order to obtain a set  $N_v$  of directions.

Secondly the image is segmented. In this case we chose the method of Canny. The operator of Canny edges is derived from the Gaussian filter. This operator approximates the segmentation operator strongly, optimizing the product of the quotients signal to noise and location [6].

Thirdly we began the Method of the Finite Element. Considering a closed enclosure the steps for the resolution are [7]:

- Divide the enclosure in Finite Elements: Triangles (3 nodes), Tetrahedrons (4 nodes), etc.
- Deduce the equation describing the potential f within an EF.
- Raise the equations giving the adjustments conditions for solutions in the EF borders.
- Calculate the potentials in the nodes of each EF by means of some of the methods that will be introduced below.
- Solve the raised algebraic equations. Generation of the finite Elements.
- Contours can be irregular
- EF will be as small as the programmer considers.
- If the potential varies a lot, the EF will consider a mesh with small "holes". It means the nodes are closer.

We propose the Energetic Function.

$$E = \sum_{i,j} \left[ p_{i,j,k} - x_{i,j,k} \right]^{2} + \lambda \left[ \sum_{i,j,k} \sum_{i_{s},j_{s},k_{s}} \left( x_{i,j,k} - x_{i_{s},j_{s},k_{s}} \right)^{2} \right]$$
enforces smoothness
$$(3)$$

Where:

 $p_{i,j,k}$  is a voxel value from the original image.

 $X_{i,j,k}$  is the classification of that voxel.

 $i_s j_s k_s$  represent the neighborhood of the voxel.

The energy is a numerical value representing a weighted summation of two main distances to the voxels taking part in the segmentation function of intensities [8]. In this study, it is desirable to make a detailed registry for all images and considering the derivates form each image structure. This can be solved by the definition of vector

field that can vary point to point in the images. In this case, the energetic function can be redefined as [9]

$$E = \sum_{i,j} \left[ p_{i,j,k} - x_{i,j,k} \right]^{2} + \lambda \left( \sum_{i,j,k} \sum_{i_{s},j_{s},k_{s}} \left( x_{i,j,k} - x_{i_{s},j_{s},k_{s}} \right)^{2} \right)$$

$$+ \left[ \lambda_{x} \lambda_{y} \lambda_{z} \right] \begin{bmatrix} \int_{\Omega} \left| \nabla u(p) \right|^{2} d\Omega \\ \int_{\Omega} \left| \nabla v(p) \right|^{2} d\Omega \\ \int_{\Omega} \left| \nabla w(p) \right|^{2} d\Omega \end{bmatrix}$$
(4)

And where the updated coordinates in the resulting image are:

$$E = \begin{bmatrix} \hat{x} \\ \hat{y} \\ \hat{z} \end{bmatrix} = \begin{bmatrix} x + u(x, y, z) \\ y + v(x, y, z) \\ z + w(x, y, z) \end{bmatrix}$$

$$= \begin{bmatrix} x + \sum_{i=1, j=1}^{m} N_{i, j, k}(x, y, z) u_{i, j, k} \\ y + \sum_{i=1, j=1}^{m} N_{i, j, k}(x, y, z) u_{i, j, k} \\ z + \sum_{i=1, j=1}^{m} N_{i, j, k}(x, y, z) u_{i, j, k} \end{bmatrix}$$
(5)

Where the interpolation or form functions  $(N_{i,j,k}(x,y,z))$  are traditionally used by

the method of finite elements for rectangular meshes [10]. In general, m is the number of total nodes depending on the number of nodes forming each element and the total number of elements which defines the mesh. Since the dominions in the images are generally of parallel sides, we have used regular lagrangians elements of 8 nodes for 3 dimensions and 4 nodes for 2 dimensions. The interpolation functions can be written easily, based on the image space. By simplicity we are going to define the system coordinate in 2 dimensions within an element anyone as it is in Figure 1 [11].

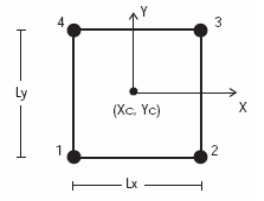


Fig. 1. - Definition of the system of coordinates.

To avoid the separate computation of the forces E, the elastic deformation, and the matching criterion, we propose to directly compute a deformation field that readily

satisfies both aspects, the elasticity constraint and a local image similarity constraint between the images to be matched ( $I_1$  and  $I_2$ ). Hence, the total energy to be minimized is expressed as:

$$E = \int_{\Omega} \lambda^{t} d\Omega + \int_{\Omega} \left( I_{1} \left( x + u \left( x, y, z \right) \right) - I_{2} \left( x, y, z \right) \right)^{2} d\Omega$$
 (6)

#### Results 3

The Figure 2 shows 3 different images of people who present anomalies and that can present fractures that cannot be, so easily detected.

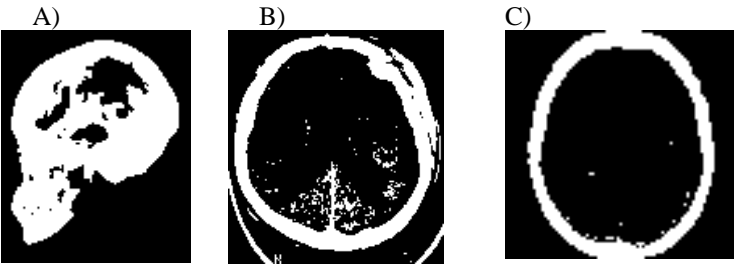


Fig. 2 Three types of encephalon analyzed by Computed Axial Tomography

In order to eliminate the image noise generated by the acquisition, in addition to initialize with the vertices of the finite element, a Gaussian filter was applied with  $\sigma = 10$  (figure 3).

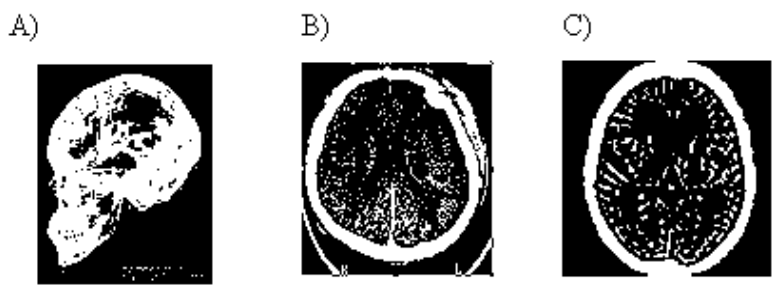


Fig. 3 Images of Skull, with Gaussian filter

To observe some details of the filtered images, an edge canny detection was used as it was stated above. Under this analysis, some relevant aspects for each figure were observed. For example, lines, among others (Figure 4).

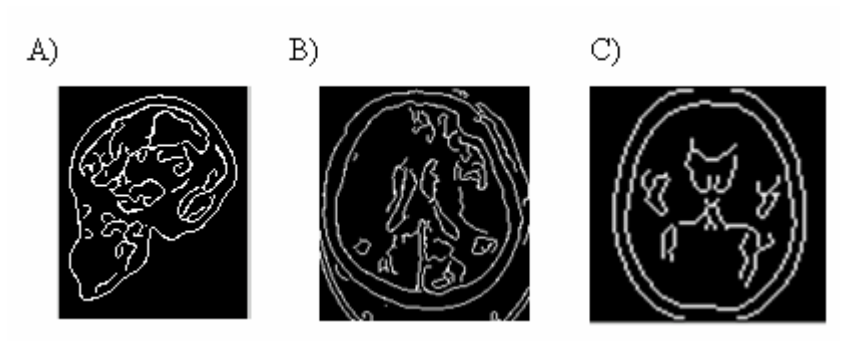
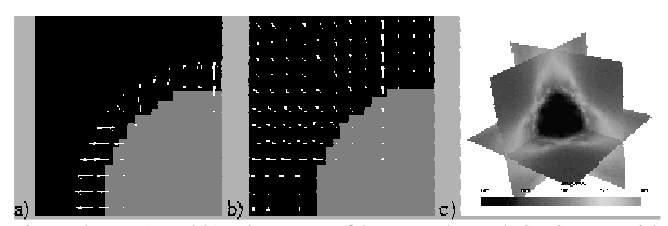
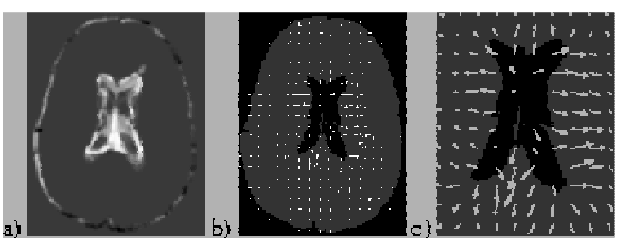


Fig. 4 Images of Skull segmented.

Also, it was applied an alternative method to show the vectors at the edge of the images (equation 1). These vectors can be helpful to design an adequate mesh to initialize the Finite Element procedure [9]. (Figures 5 y 6)



**Fig. 5**: Growing sphere. a) and b): close-ups of 2D cuts through 3D image with a) classical OF, and b) FE matching deformation fields overlaid, c) and 3D orthogonal cuts through the FE mesh with intensity coding of the displacement field. The displacement field is mainly located at the boundaries of the sphere and is propagated through the surrounding elastic medium.



**Fig. 6**: Enlarging ventricles. a) slice of difference between segmented images at both time points (gray means no difference), b) deformation field superimposed on same image at the first time point. c) close-up

In the following figures (7 and 8), it is showed the surfaces of the finite element solution. These surfaces are composed by 8 nodes and 9 elements of nodes, for the first and 16 nodes and 18 elements for the second one representing a particular zone where a fracture is located.



Fig. 7. Surface 1 of the Finite Element

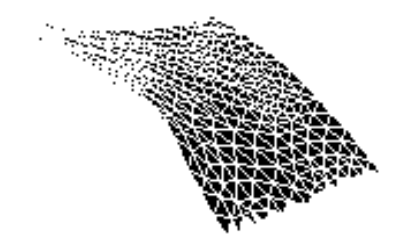


Fig. 8. Surface 2 of the Finite Element.

Once the adequate mesh (by trial and error method) has been applied to solve the finite element, it is possible to observe small details in the images that can be considered fractures (confirmed by a-priory knowledge of where the fracture is). This could be an interesting method to help physicians without experience that are not experts to detect the fractures form the magnetic resonance or computed axial tomography (Figure 9).

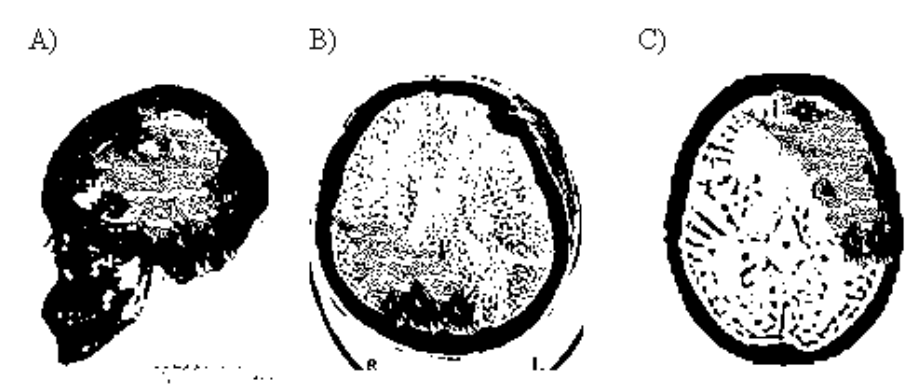


Fig. 9. Images with surface 1 of the Finite Element

With the second surface that has a large number of nodes and therefore a "better" mesh, it is possible to appreciate similar fractures (Figure 10).

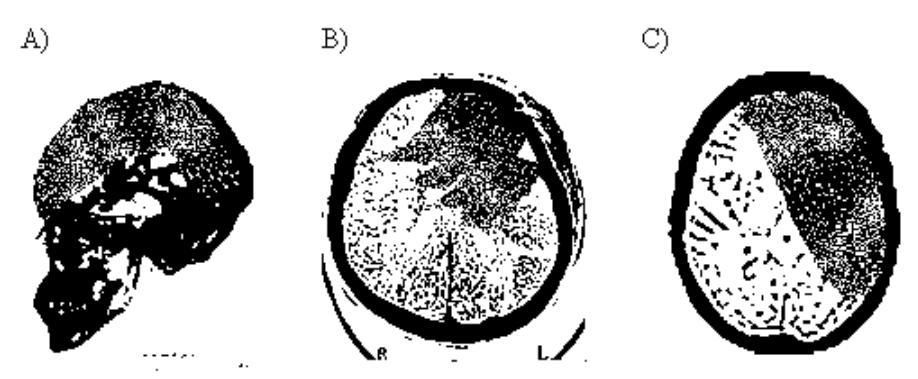


Fig. 10. Images with surface 1 of the Finite Element.

Here it is clear that a method to determine the adequate amount of nodes and the elements form must be designed. Some interesting approaches can be used to realize this aspect: the neural networks theory, the genetic algorithms, etc.

### 3 Conclusion

This paper presents a new, physics-based deformable model for tracking physical deformations (Fractures) using image matching. The model results from the minimization of a deformation field simultaneously satisfying the constraints of an elastic body and a local image similarity measure. The model provides a physically realistic deformation field and also allows us to inspect the characteristics of the deformed objects. This can be very useful for the inspection of stresses induced by the deformation of certain objects on their surroundings, in our case the detection of skull fractures.

In the experiments, the objects were considered to be homogeneous elastic bodies. Further improvements of the algorithm include the assignment of different elasticity's to the different objects represented in the image. This will require a preliminary segmentation of the objects to be deformed so as to be able to set appropriate elasticity coefficients to every cell of the mesh. Also, the anisotropy of certain skull fractures could be included into the model by modifying the elasticity matrix D appropriately.

We would lack to design an algorithm that assures that the meshes are the best possible one (in the sense of the image representation), also to include one better area within the image, providing an improvement in the diagnostic supplied by the method suggested in this manuscript.

### References

- Snell, R.. Clinical Neuroanatomy for Medical Students, Lippincott-Raven Publishers, 4<sup>th</sup> Edition (2001)
- Hauser, K. Longo, B., Jameson, F., Harrison's Principles of Internal Medicine, Mc Graw Hill. 16<sup>th</sup> Edition (2006)
- 3. Gonzalez, R. C., Woods, R.E.. Digital Image Processing. Prentice Hall, Inc.. New Jersey (2002)
- Felippa, C.A.. Introduction to finite element methods. Department of Scientist, Engine Aerospace Colorado University. Boulder, http://www.colorado.edu/engineering/CAS/courses.d/IFEM.d/Home.html.
- Ledesma, A. The Method of Finite Element Foundations for Elliptical Problems. UNAM (2006)
- Sonka, M., Hlavac, V., Boyle, R.. Image Processing, Analysis, and Machine Vision. THOMSON, USA (2006)
- 7. Passaro, A., Junior, J., Abe, N., Sasaki, M., Santos, J.. Finite-Element and Genetic Algorithm Design of Multi-segmented Electro-optic Sensor for Pulsed High-Voltage Measurement, 6th World Congresses of Structural and Multidisciplinary Optimization (2005)
- 8. Bribiesca, E., Measuring 3D shape similarity using progressive transformations. Pattern Recognition, vol. 4128, pp. 1117--1129 (1996)
- 9. Yushkevich, P., Piven, J., Cody, H., Ho, S., Gerig, G., User-Guided Level Set Segmentation of Anatomical Structures with ITK-SNAP. MICCAI Workshop, (2005)
- Brook,s R.. Model Based 3-D Interpretation of 2-D Images. IEEE Transaction Pattern Analysis Machine Intelligence, vol. 5, no.2, pp 140--150 (1983)
- 11. Galvez, J.M., Canton, M.. Normalization and shape Recognition of three-dimensional objects by 3-D Moments. Pattern Recognition, vol.26, no.5, pp.667--681 (1993)
- 12. Smith, S.. BET: Brain Extraction Tool, Technical Report. UK (2001)
- 13. Hu, M.K.. Visual Pattern Recognition by Moment Invariants. IEEE Transaction in Information Theory, vol.8, pp.179--187 (1962)